Role of Brain Tissue Localized Purine Metabolizing Enzymes in the Central Nervous System Delivery of Anti-HIV Agents 2′-β-Fluoro-2′,3′-Dideoxyinosine and 2′-β-Fluoro-2′,3′-Dideoxyadenosine in Rats

Dharmendra Singhal,[1] Michael E. Morgan,[1] and Bradley D. Anderson[1,2]

Received November 27, 1996; accepted March 4, 1997

Purpose. This study examines the central nervous system (CNS) delivery of 2′-β-fluoro-2′,3′-dideoxyadenosine (F-ddA) and 2′-β-fluoro-2′,3′-dideoxyinosine (F-ddI), acid stable analogues of dideoxyadenosine (ddA) and dideoxyinosine (ddI) having reduced susceptibility to purine salvage pathway enzymes important in the metabolism of ddA and ddI, adenosine deaminase (ADA) and purine nucleoside phosphorylase (PNP), respectively. Their CNS delivery compared to that for ddI provides insight into the role of brain tissue ADA and PNP in these processes.

Methods. Brain and cerebrospinal fluid (CSF) concentration-time profiles were obtained for F-ddI during and after intravenous infusions of F-ddI, and for both F-ddA and F-ddI after F-ddA infusions in normal rats or rats pre-treated with the ADA inhibitor 2′-deoxycoformycin (DCF). Rate constants for CNS entry, efflux and metabolism were estimated by computer fits using plasma concentration-time profiles as the driving force functions.

Results. The CNS delivery of F-ddI did not differ significantly from that for ddI. F-ddA, which is more lipophilic than F-ddI, provided higher brain (≈ 8×) and CSF (≈ 11×) concentrations of total dideoxynucleoside (F-ddA and F-ddI) compared to F-ddI. Deamination by brain tissue ADA to form F-ddI reduced CNS levels of intact F-ddA but provided higher brain parenchyma (5×) and CSF/plasma (3×) ratios of F-ddI relative to F-ddI controls. Thus, F-ddA functions in part as a CNS-activated prodrug of F-ddI. DCF pre-treatment inhibited brain tissue ADA, abolishing the prodrug effect, and enhancing F-ddA concentrations in both brain parenchyma (5×) and CSF (6×).

Conclusions. PNP metabolism does not appear to play a role in the low CNS delivery of ddI. On the other hand, deamination of F-ddA by brain tissue ADA is an important process, such that F-ddA functions in part as a CNS-activated prodrug of F-ddI. Enhanced CNS uptake of intact F-ddA can be achieved with ADA inhibition.

KEY WORDS: dideoxyadenosine; blood-brain barrier; adenosine deaminase; purine nucleoside phosphorylase; inhibitor.

INTRODUCTION

AIDS dementia complex (ADC) is a neurological disorder found in more than 60% of humans with AIDS characterized by a progressive deterioration in mental function (1,2). The pathogenesis of ADC is not well understood, however, cognitive improvement in children with symptomatic HIV infection undergoing treatment with anti-HIV agents seems to correlate with the cerebrospinal fluid (CSF)/plasma drug concentration ratio (3–6), indicating the need for agents which readily enter the central nervous system (CNS). Of the five reverse transcriptase (RT) inhibitors approved by the United States Food and Drug Administration, AZT and d4T have moderate CNS uptake with CSF/plasma drug concentration ratios of 0.2–0.3, while ddI, ddC and 3-TC exhibit very low CNS uptake, with CSF/plasma ratios of less than 0.05 (3,5–7).

Although the reason for low CNS uptake of dideoxynucleoside RT inhibitors is not well understood, metabolism by salvage pathway enzymes localized within brain tissue may play a role for some compounds. ddI, for example, is a substrate for purine nucleoside phosphorylase (PNP) (8), high activities of which are found in most mammalian cells, including erythrocytes and endothelial cells of the blood-brain barrier (BBB) (9–11). 2′,3′-Dideoxyadenosine (ddA) and its more acid stable analogue 2′-β-fluoro-2′,3′-dideoxyadenosine (F-ddA) (12,13) are readily deaminated to ddI or 2′-β-fluoro-2′,3′-dideoxyinosine (F-ddI) through the action of adenosine deaminase (ADA) (14), which is also present at high concentrations in erythrocytes, intestinal mucosa, and the BBB (11,15,16).

F-ddA is nearly 10-fold less susceptible than ddA to ADA catalyzed deamination and its hydrolysis product, F-ddI, is not a substrate for PNP (17). Moreover, approximately 5 and 20 fold higher concentrations of F-ddATP and F-ddADP were obtained in a human T-cell line *in vitro* from F-ddA compared to ddA controls (17). The acid stability and reduced deamination rate of F-ddA coupled with the PNP resistance of its deamination product, F-ddI, and its ability to undergo a more direct anabolic route to the active nucleotide intracellularly led to the consideration of F-ddA as a potentially orally bioavailable candidate for preclinical development as an anti-AIDS agent (17). F-ddA may also provide advantages in CNS delivery, as it is ≈10 times more lipophilic than F-ddI (18). However, even F-ddI, an isostere of ddI (13) with identical lipophilicity to ddI (18) may exhibit improved CNS delivery in relation to ddI, due to its PNP resistance. Although PNP is present at relatively high levels in brain capillary endothelial cells (11), its possible contribution as an enzymatic BBB for ddI has not been demonstrated. Similarly, ADA localized in cerebral capillary endothelial cells (11) may serve as an enzymatic BBB for F-ddA, leading to the formation of F-ddI during its passage into the brain (i.e., F-ddA may function as a CNS-activated prodrug of F-ddI).

In this study, the brain and CSF concentrations of F-ddI during and after intravenous (iv) F-ddI infusions, and of F-ddA and F-ddI during and after F-ddA infusions in normal rats or rats pre-treated with an ADA inhibitor, 2′-deoxycoformycin (DCF), were determined. The CNS uptake and efflux of F-ddI and ddI were compared to determine whether or not PNP resistance provides an advantage in CNS delivery. F-ddA and F-ddI concentrations in brain tissue and CSF after iv infusions of F-ddA were then explored to test the hypothesis that the 10-fold greater lipophilicity of F-ddA enhances its CNS uptake compared to F-ddI and to ascertain the extent of bioconversion of F-ddA to F-ddI in brain tissue. Finally, pre-treatment with DCF was evaluated as a means of inhibiting ADA in brain

[1] Department of Pharmaceutics and Pharmaceutical Chemistry, University of Utah, Salt Lake City, Utah 84112.

[2] To whom correspondence should be addressed. (e-mail: banderson@deans.pharm.utah.edu)

0724-8741/97/0600-0786$12.50/0 © 1997 Plenum Publishing Corporation

tissue, thereby enhancing the CNS delivery of intact F-ddA. The plasma pharmacokinetics of F-ddI and F-ddA with and without DCF pre-treatment were reported previously (19).

MATERIALS AND METHODS

Chemicals and Reagents

F-ddA, F-ddI and DCF were provided by the National Cancer Institute, National Institutes of Health (Bethesda, MD), and were used as received. ddI was obtained from the National Institute of Allergy and Infectious Diseases, National Institutes of Health, and was used without further purification. All other reagents were of analytical grade.

Experimental Designs

A total of 56 rats weighing 295 ± 6 gm (mean ± SEM) were divided into 3 separate groups. In group 1 rats (n = 18), brain tissue and CSF concentrations of F-ddI were determined during and after 2 hour iv infusions of F-ddI (48 mg/kg/hr). In group 2 animals (n = 18), brain tissue and CSF concentrations of F-ddA and F-ddI were monitored during and after 2 hour iv infusions of F-ddA (66 mg/kg/hr, dose estimated from preliminary experiments to yield concentrations of F-ddI comparable to those from a 48 mg/kg/hr F-ddI infusion) in the absence of ADA inhibition. Finally, in group 3 animals (n = 20), brain tissue and CSF concentrations of F-ddA and F-ddI were determined during and after 2 hour iv infusions of F-ddA (66 mg/kg/hr) initiated 30 min after pre-treatment with DCF (1 mg/kg). Plasma samples were also taken from the above groups of animals and analyzed in a separate study (19).

Drug Infusion and Sampling Protocols

Male Sprague-Dawley rats obtained from Sasco Laboratories (Omaha, NE) were housed and cared for at the Animal Resource Center, University of Utah, according to the USDA Animal Welfare Act and the NIH Guide for the Care and Use of Laboratory Animals. Abdominal aorta (AA) and inferior vena cava (IVC) cannulas were implanted for drug administration and collection of blood samples as described earlier (19).

The protocol for drug infusion and collection of plasma samples has been described in a previous paper reporting the pharmacokinetics of these compounds. After blood samples were taken, rats were sacrificed to obtain CSF and brain tissue. CSF samples were obtained by cisterna magna puncture using a 24-gauge needle attached to silastic tubing (20). After withdrawal of CSF, animals were quickly decapitated to obtain brain tissue. Both CSF and brain samples were immediately frozen in liquid nitrogen and stored at −70°C prior to HPLC analyses.

Sample Preparation and HPLC Analysis

Frozen brain tissue was thawed, weighed and homogenized in 1.5 ml water. Acetonitrile (12 ml) was added to precipitate proteins and the samples were vortexed, centrifuged and re-extracted with 0.5 ml water and 2 ml acetonitrile. The combined supernatants were evaporated to dryness under nitrogen, reconstituted in 0.6 ml phosphate buffer (I = 0.02, pH 7.4 for F-ddI samples or pH = 2.0 for F-ddA containing samples), and filtered (0.45 μm nylon filters) before HPLC analysis. CSF samples were thawed, diluted if necessary and analyzed directly by HPLC.

F-ddI and F-ddA in brain tissue or CSF were determined by reverse-phase HPLC (Supelcosil LC-18S 5μ column, 4.6 mm i.d. × 25 cm) with UV detection at 260 nm. Analyses of F-ddI alone utilized mobile phases containing 4% methanol in phosphate buffer (pH = 5.0; I = 0.02) for brain tissue or 8% methanol in phosphate buffer (pH = 3; I = 0.02) for CSF yielding retention volumes of 38 and 14 ml, respectively. Samples containing both F-ddI and F-ddA were analyzed using 4% methanol with 0.01% tetrabutylammonium ion in phosphate buffer (I = 0.01, pH = 4 for brain tissue, pH = 2.5 for CSF). The retention volumes of F-ddI were 40 and 18 ml, while those for F-ddA were 78 and 8 ml, respectively, in these mobile phases. Recoveries of F-ddI from spiked brain and CSF averaged 96 ± 4% (mean ± SD, n = 4) and 101 ± 2% (mean ± SD, n = 3), respectively. Recoveries of F-ddA were 97 ± 3% (mean ± SD, n = 3) and 99 ± 2% (mean ± SD, n = 3) in spiked brain and CSF samples, respectively.

Data Analyses

Plasma concentration-time profiles from groups 1–3 were analyzed in a separate study (19). Parameters obtained from these data were used to generate fitted plasma concentrations, C_{plasma}, needed for the input function for CNS entry in the equations below. CNS (i.e., brain parenchyma or CSF) concentration-time profiles of F-ddI during and after F-ddI infusions or literature data for ddI CNS concentration-time profiles during and after ddI infusions (7) were analyzed using a compartmental model as depicted for F-ddI in Eq. (1):

$$\frac{dC_{CNS}^{F-ddI}}{dt} = k_{in}^{F-ddI} C_{plasma}^{F-ddI} - k_{out}^{F-ddI} C_{CNS}^{F-ddI} \quad (1)$$

where k_{in} and k_{out} are the apparent rate constants for entry and efflux, respectively, of drug into and out of brain parenchymal tissue or CSF and C_{CNS} is the concentration of drug in either CSF or brain parenchyma after correction for a vascular contribution to the total drug concentration in brain tissue.

Compartmental models for F-ddI and F-ddA concentrations in groups 2 and 3 allowed for the possibility of ADA catalyzed deamination of F-ddA within the CNS via inclusion of a first-order bioconversion rate constant, k_{ADA}, in Eqns. (2) and (3). Using Eqns. (1)–(3), the concentration-time

$$\frac{dC_{CNS}^{F-ddA}}{dt} = k_{in}^{F-ddA} C_{plasma}^{F-ddA} - k_{out}^{F-ddA} C_{CNS}^{F-ddA} - k_{ADA} CD_{CNS}^{F-ddA} \quad (2)$$

$$\frac{dC_{CNS}^{F-ddI}}{dt} = k_{n}^{F-ddI} C_{plasma}^{F-ddI} - k_{out}^{F-ddI} C_{CNS}^{F-ddI} + k_{ADA} C_{CNS}^{F-ddA} \quad (3)$$

profiles from all groups were fit simultaneously by nonlinear regression analysis to determine a single set of self-consistent parameters. Because some parameters were shared for more than a single profile, the statistics were markedly improved by this approach. Error estimates were also improved when the parameters fitted were k_{out} and the transformed parameter k_{in}/k_{out} rather than k_{in}. Assumptions necessary to treat the data in this manner were the following: (a) the effective vascular volume (V_s) within brain tissue is the same for all compounds;

(b) the brain tissue distribution volumes of F-ddI and F-ddA are identical; and (c) transport parameters for F-ddA and F-ddI were unaffected by the presence of the other and unchanged in DCF pre-treated rats. The areas under the fitted brain tissue and CSF concentration-time profiles to the last time point (AUC) were normalized to the plasma AUCs reported previously (19) to obtain $AUC_{tissue/plasma}$ ratios. Statistical analyses were performed using Student's t-tests; p values of <0.05 were considered statistically significant.

RESULTS

CNS Delivery of FddI After FddI Infusion (Group 1)

Semilogarithmic plots of the F-ddI brain tissue concentrations (C_{brain}) and CSF concentrations (C_{CSF}) normalized to the steady-state plasma concentration ($C_{s.s.\ plasma}$) versus time during and after a 120-min infusion of F-ddI (group 1) are shown in Fig. 1. C_{brain} and C_{CSF} for F-ddI increased slowly with infusion time, approaching but not reaching steady-state during the 120-min infusions. At 120 min, brain tissue and CSF concentrations were only 3.3 ± 1.1% and 1.1 ± 0.1% (mean ± SD, n = 2), respectively, of plasma concentrations. The solid lines in Fig. 1 represent computer fits of the pooled data and the parameters generated are listed in Table 1.

Also displayed in Fig. 1 are the profiles for $C_{brain}/C_{s.s.\ plasma}$ and $C_{CSF}/C_{s.s.\ plasma}$ versus time for ddI, determined previously in these laboratories (7,21). The concentrations of ddI in brain and CSF reached steady-state within 30 min of the start of infusions, attaining plateau values of 4.3 ± 2.6% (n = 5) and 1.6 ± 1.2% (n = 3) of plasma ddI concentrations, respectively. The solid lines in Fig. 1 represent computer fits of the pooled data. Table 1 lists the parameters generated from these fits. The most reliable parameter for comparing CNS uptake is the k_{in}/k_{out} ratio. These values were the same for ddI and F-ddI indicating that PNP must not play an important role in the CNS uptake of ddI.

Table 2 summarizes the steady-state tissue/plasma concentration ratios for both ddI and F-ddI in brain tissue and CSF. These ratios are compared in Table 2 to the computer fitted k_{in}/k_{out} ratios and to $AUC_{tissue}/AUC_{plasma}$ ratios. The k_{in}/k_{out} ratios match the steady-state CSF/plasma concentration ratios closely, confirming that steady-state was indeed attained. The brain tissue/plasma concentration ratios exceed k_{in}/k_{out} due to the vascular contribution within brain tissue. The fitted value of the vascular space within brain tissue is 2.3% of the brain tissue volume.

CNS Delivery of F-ddA and F-ddI During and After F-ddA Infusions

The CNS delivery of F-ddA administered iv and its conversion *in vivo* to F-ddI by ADA in the systemic circulation and in the CNS were examined in group 2. Concentration-time profiles of F-ddA and F-ddI formed *in vivo* after F-ddA infusions are shown in Fig. 2. The steady-state concentrations of intact F-ddA in brain tissue and CSF after an iv infusion of F-ddA were 5 ± 1% and 9 ± 2%, respectively, of the steady-state plasma concentration. However, the concentrations of F-ddI in the CNS exceeded those of F-ddA itself, indicating significant bioconversion of F-ddA to F-ddI. After correcting

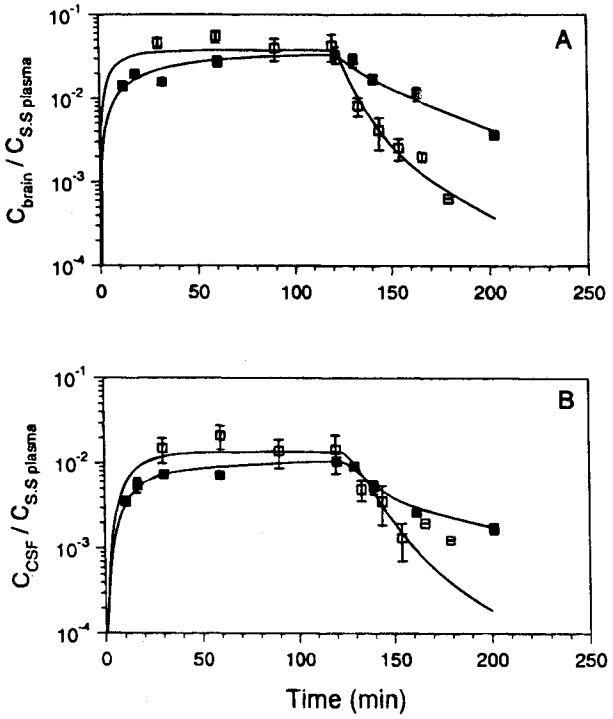

Fig. 1. Brain (A) and CSF (B) concentration-time profiles (mean ± SEM, n = 2) of F-ddI (■) and ddI (□) obtained after 120-min infusion of F-ddI or ddI in rats. Concentrations were normalized to steady-state plasma concentrations. Solid lines show the computer fit of the pooled data according to eqns. [1–3].

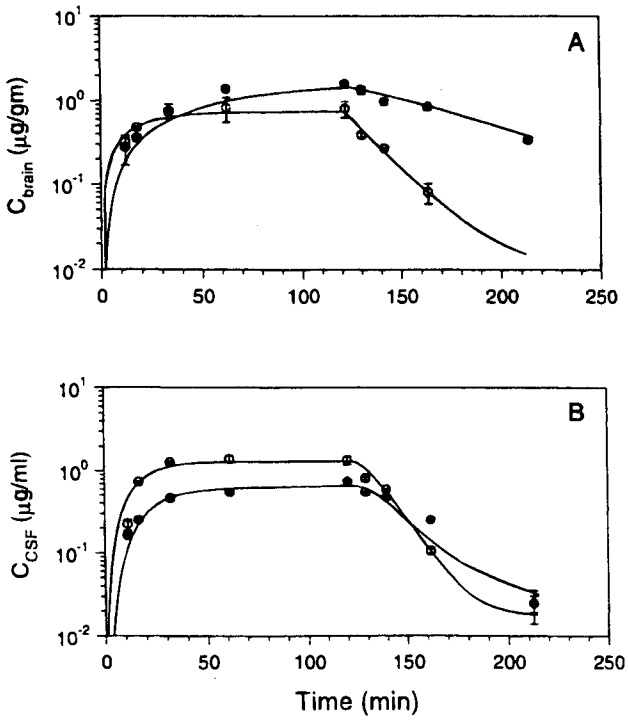

Fig. 2. Brain (A) and CSF (B) concentration-time profiles (mean ± SEM, n = 2) of F-ddA (○) and F-ddI (●) formed in vivo after 120-min infusion of F-ddA infusion (66 mg/kg/hr) in rats. Solid lines show the computer fit of the pooled data according to eqns. (1–3).

Table 1. Kinetic Parameters Obtained from Nonlinear Regression Analysis of the Pooled Brain Tissue and CSF Concentration vs. Time Data for ddI After 120-min ddI Infusion (125 mg/kg/hr), F-ddI After 120-min F-ddI Infusion (48 mg/kg/hr), and F-ddA and F-ddI After 120-min F-ddA Infusion (66 mg/kg/hr) in Normal or DCF Treated Rats

Tissue	Parameter[a]	ddI	F-ddI	F-ddA
Brain	k_{in}/k_{out} ($\times 10^2$)	1.4 ± 0.4	0.9 ± 0.2	8.3 ± 0.7
	k_{out}[b]	0.11 ± 0.03	0.024 ± 0.004	0.020 ± 0.004
	k_{ADA}[b]	NA[c]	NA[c]	0.042 ± 0.006
	k_{ADA}(with DCF)[b]	ND[d]	ND[d]	ND[d]
	V_s[e](%)	2.3 ± 0.2	2.3 ± 0.2	2.3 ± 0.2
CSF	k_{in}/k_{out} ($\times 10^2$)	1.4 ± 0.2	1.03 ± 0.07	20 ± 2
	k_{out}[b]	0.10 ± 0.02	0.17 ± 0.03	0.035 ± 0.006
	k_{ADA}[b]	NA[c]	NA[c]	0.058 ± 0.009
	k_{ADA}(with DCF)[b]	NA[c]	NA[c]	0.0032 ± 0.0007

[a] Value of estimate ± SD of estimate.
[b] min^{-1}.
[c] Not applicable.
[d] Not determined (F-ddI not detected).
[e] Shared between ddI, F-ddI and F-ddA.

for a vascular contribution (2.3% of the total brain tissue volume), the brain parenchyma/plasma and CSF/plasma concentration percentages of total dideoxynucleoside (F-ddA and F-ddI) were 7.7% and 12.1%, respectively, ≈8 and ≈11 fold higher than the values obtained for F-ddI after F-ddI infusion.

The solid lines in Fig. 2 show computer fits of Eqs. [2] and [3] to the pooled data. Parameters obtained from these fits are listed in Table 1. The parameter values indicate that F-ddA is converted to F-ddI with apparent first-order rate constants of 0.042 ± 0.006 min^{-1} and 0.058 ± 0.009 min^{-1} in brain tissue and CSF, respectively. While these values are not significantly different from each other as judged by their 95% confidence intervals they are statistically different from zero ($p < 0.05$).

Fig. 3 displays the brain tissue and CSF concentrations of F-ddI normalized to the steady-state plasma F-ddI concentration formed *in vivo* after F-ddA infusions. Similar profiles for F-ddI after F-ddI infusions (group 1) are also shown in Fig. 3. The ratios $C_{brain}/C_{s.s.\ plasma}$, $C_{parenchyma}/C_{s.s.\ plasma}$, and $C_{CSF}/C_{s.s.\ plasma}$ for F-ddI after F-ddA infusion are approximately 2-, 5- and 3- fold higher, respectively, than those obtained from infusions of F-ddI, again suggesting that bioconversion of F-ddA to F-ddI in the CNS was significantly greater than zero. Thus, F-ddA functions in part as a prodrug of F-ddI for enhancing the delivery of F-ddI to the CNS.

Effect of DCF Treatment on CNS Delivery of FddA

The concentration-time profiles for F-ddA and F-ddI formed *in vivo* after F-ddA infusions in normal (group 2) or DCF treated (group 3) rats are shown in Fig. 4. The solid lines in Fig. 4 represent computer fits of the pooled data using Eqs. [2] & [3]. Fitting all data sets both with and without ADA inhibitor resulted in dramatic improvement in parameter estimates (Table 1), particularly in the estimates of k_{out} and k_{ADA} for F-ddA. DCF pre-treatment was highly effective in inhibiting brain tissue ADA, as F-ddI could no longer be detected in brain tissue from DCF pre-treated rats. The higher sensitivity of the F-ddI assay in CSF allowed the detection of low levels of F-ddI in CSF (Fig. 4), making possible the estimation of an apparent bioconversion rate constant after DCF pre-treatment. The value obtained (Table 1) suggests that approximately 94% of the brain tissue ADA activity was abolished by DCF pre-treatment.

Table 2 summarizes the steady-state tissue/plasma concentration ratios for both F-ddI and F-ddA in brain tissue and CSF both with and without DCF pre-treatment. (In DCF pre-treated

Table 2. Parameters for Measuring the Extent of CNS Uptake of ddI After 120-min ddI Infusion (125 mg/kg/hr), F-ddI After 120-min F-ddI Infusion (48 mg/kg/hr), and F-ddA and F-ddI After 120-min F-ddA Infusion (66 mg/kg/hr) in Normal or DCF Treated Rats

			F-ddI		F-ddA	
Tissue	Parameter[a]	ddI	After F-ddI	After-FddA	No DCF	After DCF
Brain	$C_{s.s.\ brain}/C_{s.s.\ plasma}$ (%)	4 ± 1	3.3 ± 0.8	7 ± 1[b]	5.0 ± 0.5	7 ± 1[b]
	$C_{s.s.\ parenchyma}/C_{s.s.\ plasma}$ (%)	1.7 ± 1	1.0 ± 0.8	4.7 ± 1[b]	2.7 ± 0.5	4.7 ± 1[b]
	k_{in}/k_{out} ($\times 10^2$)[c]	1.4 ± 0.4	0.9 ± 0.2	0.9 ± 0.2	8.3 ± 0.7	8.3 ± 0.7
	AUC_{brain}/AUC_{plasma} (%)	3.8	3.1	8.8	3.3	9.4
CSF	$C_{s.s.CSF}/C_{s.s.\ plasma}$ (%)	1.6 ± 0.7	1.1 ± 0.1	3.4 ± 0.4	9 ± 1	17.6 ± 0.8[b]
	k_{in}/k_{out} ($\times 10^2$)[c]	1.4 ± 0.2	1.03 ± 0.07	1.03 ± 0.07	20 ± 2	20 ± 2
	AUC_{CSF}/AUC_{plasma} (%)	1.4	1.1	4.1	5.0	18.8

[a] Value ± SEM (n = 2–6).
[b] Concentration at 120 min did not reach steady-state.
[c] Determined from pooled data.

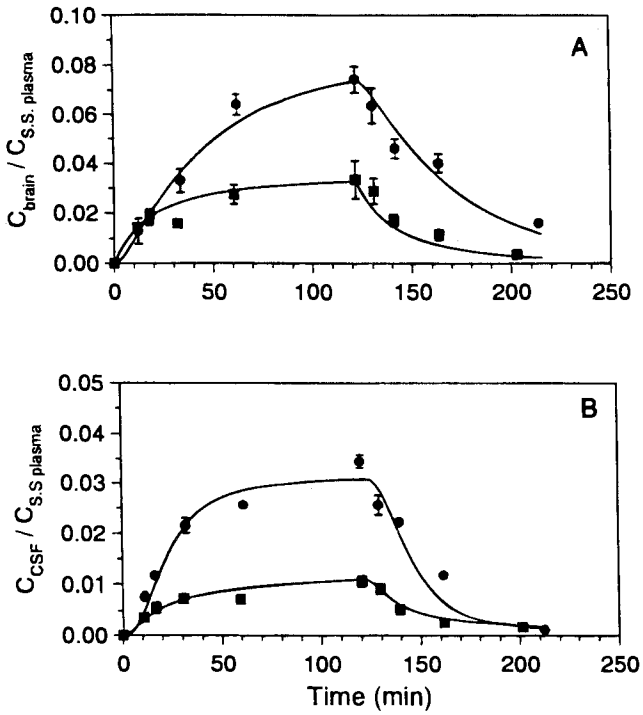

Fig. 3. Brain (A) and CSF (B) concentration-time profiles (mean ± SEM, n = 2) of F-ddI obtained after 120-min infusion of F-ddI (■) or F-ddA (●) in rats without ADA inhibition. Concentrations were normalized to steady-state plasma concentrations of F-ddI. Solid lines show the computer fit of the pooled data according to eqns. (1–3).

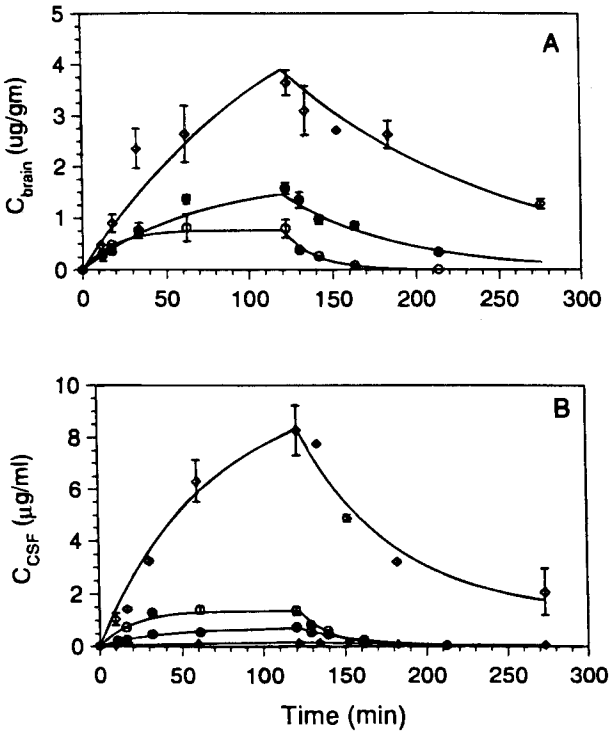

Fig. 4. Brain (A) and CSF (B) concentration-time profiles (mean ± SEM, n = 2) of F-ddA (open symbols) and F-ddI (filled symbols) after F-ddA infusion (66 mg/kg/hr) in normal (circles—○, ●) or DCF treated (diamonds—◇, ◆) rats. Solid lines show the computer fit of the pooled data according to eqns. (1–3) .

animals, F-ddA concentrations did not quite reach steady-state (Fig. 4). The ratios reported are those determined at the 120 min time points.) As described previously for ddI and F-ddI, these ratios are compared in Table 2 to the computer fitted k_{in}/k_{out} ratios and to $AUC_{tissue}/AUC_{plasma}$ ratios. The k_{in}/k_{out} ratios for F-ddA are significantly greater than the steady-state CSF/plasma concentration ratios in rats not pre-treated with DCF, while those for F-ddI are smaller than the steady-state CSF/plasma concentrations, reflecting the effects of ADA metabolism. Similar patterns hold in brain tissue after allowing for the 2.3% vascular contribution to the brain tissue/plasma percentages. DCF pre-treatment resulted in 120 min CSF/plasma concentration ratios approaching the k_{in}/k_{out} ratios. Similarly, brain tissue/plasma concentration ratios approached k_{in}/k_{out} after correction for the brain tissue vascular term.

In group 2, the steady-state concentrations of F-ddA in brain tissue and CSF after an iv infusion of F-ddA in DCF untreated rats were 0.8 ± 0.2 µg/gm in brain tissue and 1.3 ± 0.1 µg/ml in CSF, respectively. In comparison, as shown in Fig. 4, the concentrations of F-ddA in the brain and CSF after a 120 min. iv infusion of F-ddA in DCF treated rats were 3.2 ± 0.5 µg/gm brain and 8.3 ± 1.4 µg/ml CSF, respectively, though not yet at steady-state. Thus, DCF administration increased C_{brain}, $C_{parenchyma}$, and C_{CSF} for F-ddA at 120 min by 4 ± 1, 5 ± 2 and 6 ± 1 fold, respectively. The effects of ADA inhibition on C_{brain}, $C_{parenchyma}$, and C_{CSF} normalized to $C_{s.s. plasma}$ for F-ddA are displayed in Fig. 5 (panel A). Also shown (panel B) are calculated values of the enhancement of F-ddA levels at 120 min in various tissues due to ADA inhibition. These comparisons illustrate that the substantial increases in F-ddA concentrations in the CNS were primarily due to ADA inhibition in plasma, which increased plasma F-ddA concentrations by 2.9 fold. Inhibition of brain tissue ADA further elevated brain parenchymal and CSF concentrations of F-ddA by 1.8 and 2.0-fold, respectively.

DISCUSSION

CNS Delivery of F-ddI and ddI—The Role of PNP

Previous studies in this laboratory have shown that at steady-state the CNS concentrations of ddI are very low relative to plasma concentrations (7,21). Plausible reasons for the apparent exclusion of ddI from the brain and CSF are: (a) metabolism of ddI in brain tissue; and (b) active transporters/efflux pumps (7). ddI is susceptible to PNP catalyzed glycosidic bond cleavage, resulting in the formation of inactive hypoxanthine. We have previously shown that enzymatic degradation of ddI by PNP accounts for approximately 70% of the total systemic clearance of ddI in rats (19). Since high activities of PNP are also found in endothelial cells of the BBB (11), we speculated that PNP might account for the reduced steady-state concentrations of ddI in the CNS.

The two analogues, F-ddI and ddI have nearly identical physico-chemical properties, except for their acid lability and susceptibility to PNP. Marquez *et al* noted that the van der Waals radius of fluorine (1.35 Å) closely resembles that of hydrogen (1.20 Å), so substitution of fluorine for hydrogen

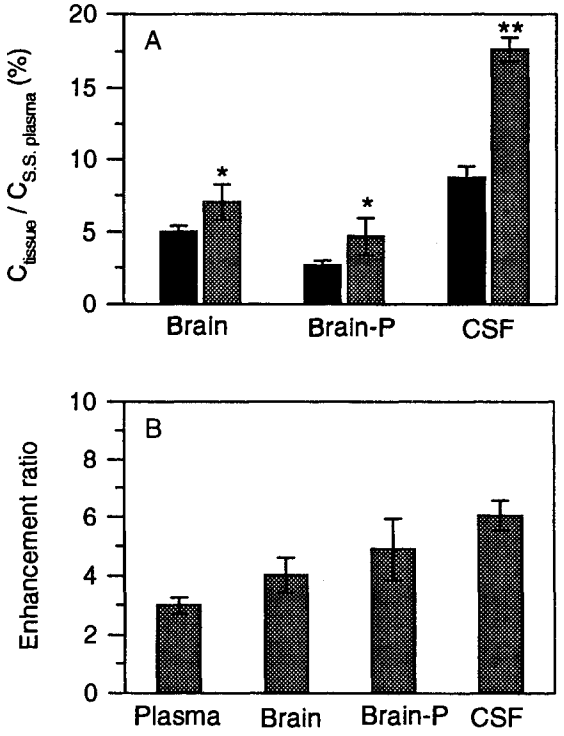

Fig. 5. Steady-state concentrations of F-ddA in brain, brain-parenchyma and CSF normalized to plasma concentration of F-ddA after F-ddA infusion in normal (mean ± SEM, n = 6, filled bars) or DCF treated (mean ± SEM, n = 2, shaded bars) rats (A). Brain/plasma and brain-P/plasma ratios were statistically higher in DCF treated rats than that obtained in normal rats with $p < 0.1$ (*) while the CSF/Plasma ratio was found to be higher at $p < 0.05$ (**). Panel B shows the enhancement in concentrations of F-ddA in plasma, brain, brain-P and CSF due to DCF treatment.

should minimally perturb receptor or enzyme binding (13). Moreover, F-ddI and ddI have virtually identical octanol/water partition coefficients (18). Thus a comparison of the CNS delivery of F-ddI (a non-PNP substrate) with that of ddI may reveal the role of PNP in restricting the entry of ddI into the CNS.

As shown in Fig. 1, the brain/plasma and CSF/plasma concentration ratios of F-ddI and ddI appear to approach the same steady-state value, within experimental error, suggesting that PNP localized in brain tissue does not play an important role in the CNS uptake of ddI, in contrast to its importance in the systemic elimination of ddI. The brain tissue and CSF concentrations of ddI reached steady-state within 30 min after the start of ddI infusions, more rapidly than F-ddI, while the decline in the CNS concentrations of F-ddI after the termination of infusions was slower than for ddI (Fig. 1). These apparent differences, however, reflect primarily differences in plasma pharmacokinetics (19).

Consistent with the above finding that PNP within the BBB does not limit the CNS entry of ddI, the k_{in}/k_{out} ratios for F-ddI were not significantly different (Table 2). Johnson and Anderson have previously suggested that PNP, though present at relatively high activities in bovine brain capillary endothelial cells would not likely constitute an enzymatic BBB for ddI because of the relatively low V_{max}/K_m for ddI in the presence of this enzyme (11). The similarities in the CNS delivery of F-ddI and ddI appear to support this contention.

CNS Delivery of F-ddA—Bioconversion to F-ddI by Brain Tissue Localized ADA

The CNS uptake of dideoxynucleosides seems to correlate qualitatively with their octanol-water partition coefficients, with the moderately lipophilic agent AZT ($P_{octanol/water}$ = 1.0) exhibiting moderate CNS uptake while ddI ($P_{octanol/water}$ = 0.06) and ddC ($P_{octanol/water}$ = 0.05) exhibit low CNS entry (3,5–7). F-ddA ($P_{octanol/water}$ = 0.66) is approximately 10-times more lipophilic than F-ddI and hence might be expected to exhibit much higher CNS uptake. However, the CNS uptake of intact F-ddA may be decreased substantially if it is converted to F-ddI by ADA localized in the brain tissues. Substantial levels of ADA exist in brain tissue, with particularly high activities in endothelial cells of the BBB(11,15,16). Although F-ddA has a lower V_{max} and larger K_m than ddA, leading to a V_{max}/K_m which is at least 10-fold smaller than that for ddA (18), it has nevertheless been shown to be rapidly converted to F-ddI in the systemic circulation (19).

Fig. 5 shows that the CNS uptake of F-ddA is low, with only 5% and 9% of the plasma concentration of F-ddA present in the brain tissue and CSF, respectively, at steady-state (120 min). As shown in Fig. 2, however, the concentrations of F-ddI in brain tissue exceeded those of F-ddA itself. Substantial F-ddI concentrations were also found in CSF though less than the concentration of F-ddA. Elevated tissue/plasma ratios of F-ddI in both brain tissue and CSF when F-ddA, rather than F-ddI, was the drug infused suggests that bioconversion occurs not only in the systemic circulation but in brain tissue as well. Due to possible bioconversion of F-ddA to F-ddI by ADA localized in the CNS, the sum of F-ddA and F-ddI concentrations in the CNS after F-ddA infusions needs to be considered in assessing the effect of the increased lipophilicity of F-ddA on its CNS uptake. After 120 min-infusions, the total dideoxynucleoside (F-ddA plus F-ddI) brain parenchyma/plasma concentration and CSF/plasma concentration ratios were ≈8 and ≈11 fold higher than those obtained for F-ddI after F-ddI infusions. These findings are consistent with the expected effect of lipophilicity in enhancing the CNS uptake of F-ddA.

A significant portion of F-ddI present in the CNS after F-ddA infusion may have come from F-ddI formed systemically, where approximately 58% of administered F-ddA has been shown to convert to F-ddI in rats. This contribution needs to be factored out from the contribution of brain tissue bioconversion of F-ddA in interpreting the elevated CNS concentrations of F-ddI. Using Eqns. [2] & [3], the values of k_{ADA} in Table 1 were obtained. These values are significantly greater than zero, confirming than F-ddA → F-ddI bioconversion occurs in brain tissue. Estimates of k_{ADA} appear to be smaller than that for F-ddA systemic hydrolysis (0.087 min^{-1}) reported previously (19), though of similar magnitude.

Several strategies have been proposed to increase the CNS delivery of anti-AIDS nucleoside RT inhibitors, including the prodrug approach (22), chemical-delivery systems (23,24) and others. Of these, lipophilic ADA activated prodrugs such as the 6-halogenated congeners of 2′,3′-dideoxypurine nucleosides seem to be among the most promising for the delivery of ddI to the brain. Due to the relatively high ADA activity in rat brain tissue (which is also the case in human brain tissue), iv infusions of 6-Cl-2′,3′-dideoxypurine, an ADA activated prodrug of ddI, resulted in a 10-fold increase in brain parenchy-

mal concentrations of ddI relative to a ddI control infusion (22,25). F-ddA would be expected to function similarly as a prodrug of F-ddI with enhanced CNS delivery as it is also an ADA substrate and approximately 10-fold more lipophilic than F-ddI.

The brain-, brain parenchyma- and CSF/plasma concentration ratios of F-ddI after F-ddA infusion were found to be about 2-, 5- and 3-fold higher than those obtained after F-ddI infusions, clearly indicating that F-ddA is acting as a CNS-activated prodrug of F-ddI.

CNS Uptake of F-ddA and FddI After F-ddA Infusion in DCF-Treated Rats

The conversion of dideoxynucleoside RT inhibitors to their triphosphates is essential for their termination of viral DNA helix synthesis (26–28). There are two routes of formation of ddATP or F-ddATP from ddA or F-ddA: direct phosphorylation or an indirect pathway involving intracellular deamination followed by monophosphate formation, reamination and ultimate conversion to F-ddATP or ddATP. The conversion of dideoxynucleosides to their active triphosphates is slow (29) and must compete with other elimination pathways. Due to these catabolic routes and competition with other nucleosides for phosphorylation, very low concentrations of ddATP are generated intracellularly. Since F-ddA is less susceptible to ADA-catalyzed deamination than ddA, about 5-fold higher concentrations of F-ddATP were found in MOLT-4 cells relative to ddA controls (17). Significant further enhancement in the intracellular F-ddATP concentrations has been achieved in MOLT-4 cells by treatment with DCF, a potent inhibitor of ADA, at concentrations sufficient to inhibit primarily extracellular ADA (14). These findings suggest that increasing F-ddA concentrations in poorly accessible tissues, such as the CNS, may lead to higher concentrations of F-ddATP intracellularly. We were also interested in inhibiting ADA to better estimate the CNS influx and efflux rate constants of F-ddA and F-ddI, since k_{out} for F-ddA was found to be highly correlated (inverse correlation) with k_{ADA} in group 2 experiments making a reliable estimate of both parameters difficult to obtain.

As shown in Table 2, at 120 min the brain tissue/plasma and CSF/plasma concentration ratios of F-ddA in DCF treated rats increased to 7% and 18%, respectively, 1.4-fold and 2.0-fold higher than in normal rats. DCF administration increased the F-ddA concentrations in brain tissue, brain parenchyma and CSF by 4 ± 1, 5 ± 2 and 6 ± 1 fold, respectively, while reducing F-ddI concentrations to nearly undetectable levels. These findings indicate nearly complete inhibition of ADA and imply that combinations of F-ddA with an ADA inhibitor may provide significant advantages in reducing the clinical dosage required to achieve antiviral effect, providing that adequate safety can be realized and that F-ddA is in fact the preferred agent for CNS delivery.

ACKNOWLEDGMENTS

We thank Drs. James Kelley and John Driscoll, National Cancer Institute for providing F-ddI and for helpful discussions. This study was supported by NIH grant AI34133.

REFERENCES

1. R. W. Price and B. J. Brew J. *Infect. Dis.* **158**:1079–1083 (1988).
2. R. W. Price. *Res. Publ. Assoc. Res. Nerv. Ment. Dis.* **72**:1–45 (1994).
3. K. M. Butler, R. N. Husson, F. M. Balis, P. Brouwers, J. Eddy, D. El-Amin, J. Gress, M. Hawkins, P. Jarosinski, H. Moss, D. Poplack, S. Santacroce, D. Venzon, L. Wiener, P. Wolters, and P. A. Pizzo. *New Engl. J. Med.* **324**:137–144 (1991).
4. P. A. Pizzo, K. Butler, F. Balis, E. Brouwers, M. Hawkins, J. Eddy, M. Einloth, J. Falloon, R. Hussan, P. Jarosinski, J. Meer, H. Moss, D. G. Poplack, S. Santacrose, L. Wiener, and P. Wolters. *J. Pediatr.* **117**:799–808 (1990).
5. P. A. Pizzo, J. Eddy, J. Falloon, F. M. Balis, R. F. Murphy, H. Moss, P. Wolters, P. Brouwers, P. Jarosinski, M. Rubin, S. Broder, R. Yarchoan, A. Brunett, M. Maha, S. Nusinhoff-Lehrman, and D. G. Poplack. *N. Engl. J. Med.* **319**:889–896 (1988).
6. E. Sandstrom and B. Oberg. *Drugs* **45**:488–508 (1993).
7. B. D. Anderson, B. L. Hoesterey, D. C. Baker, and R. E. Galinsky. *J Pharmacol. Exp. Ther.* **253**:113–118 (1990).
8. D. J. Back, S. Ormesher, J. F. Tjia, and R. Macleod. *Br. J. Clin. Pharmacol.* **33**:319–322 (1992).
9. R. E. Parks, Jr., G. W. Crabtree, C. M. Kong, R. P. Agarwal, K. C. Agarwal, and E. M. Scholar. *Ann. N.Y. Acad. Sci.* **255**:412–434 (1975).
10. G. Mistry and G. I. Drummond. *J. Mol. Cell Cardiol.* **18**:13–22 (1986).
11. M. D. Johnson and B. D. Anderson. *Pharm. Res.* **13**:1881–1886 (1996).
12. V. E. Marquez, C. K.-H. Tseng, J. A. Kelley, H. Mitsuya, S. Broder, J. S. Roth, and J. S. Driscoll. *Biochem. Pharmacol.* **36**:2719–2722 (1987).
13. V. E. Marquez, C. K.-H. Tseng, H. Mitsuya, S. Aoki, J. A. Kelley, J. Ford, H., J. S. Roth, S. Broder, D. G. Johns, and J. S. Driscoll. *J. Med. Chem.* **33**:978–985 (1990).
14. G. S. Ahluwalia, D. A. Cooney, T. Shirasaka, H. Mitsuya, J. S. Driscoll, and D. G. Johns. *Mol. Pharmacol.* **46**:1002–1008 (1994).
15. C. L. Zielke and C. H. Suelter. In P. D. Boyer, (ed.) *The Enzymes,* Academic, London, 1971, vol. 4, pp. 47–78.
16. T. G. Brady and C. I. O'Donovan. *Comp. Biochem. Physiol.* **14**:101–120 (1965).
17. R. Masood, G. S. Ahluwalia, D. A. Cooney, A. Fridland, V. E. Marquez, J. S. Driscoll, Z. Hao, H. Mitsuya, C. F. Perno, S. Broder, and D. G. Johns. *Mol. Pharmacol.* **37**:590–6 (1990).
18. J. J. Barchi, Jr., V. E. Marquez, J. S. Driscoll, H. Ford, Jr., H. Mitsuya, T. Shirasaka, S. Aoki, and J. A. Kelley. *J. Med. Chem.* **34**:1647–1655 (1991).
19. D. Singhal, M. E. Morgan, and B. D. Anderson. *Drug Metab. Disp.* **24**:1155–1161 (1996).
20. H. B. Waynforth. *Experimental and Surgical Techniques in the Rat,* Academic Press, London, 1980.
21. R. E. Galinsky, K. K. Flaharty, B. L. Hoesterey, and B. D. Anderson. *J. Pharmacol. Exp. Ther.* **257**:972–978 (1991).
22. B. D. Anderson, R. E. Galinsky, D. C. Baker, S.-C. Chi, B. L. Hoesterey, M. E. Morgan, K. Murakami, and H. Mitsuya. *J. Control. Rel.* **19**:219–230 (1992).
23. M. E. Brewster, W. R. Anderson, D. O. Helton, N. Bodor, and E. Pop. *Pharm. Res.* **12**:796–798 (1995).
24. M. E. Brewster, W. Anderson, and N. Bodor. *J. Pharm. Sci.* **80**:843–846 (1991).
25. M. E. Morgan, S.-C. Chi, K. Murakami, H. Mitsuya, and B. D. Anderson. *Antimicrob. Agents Chemother.* **36**:2156–2165 (1992).
26. N. Clumeck. *J. Antimicrob. Chemother.* **32**:133–138 (1993).
27. H. Mitsuya, R. Yarchoan, and S. Broder. *Sci.* **249**:1533–1544 (1990).
28. H. Mitsuya and S. Broder. In R. C. Gallo, G. Jay, (ed.) *The Human retoviruses,* Academic Press, Inc., San Diego, 1991, 335–378.
29. D. A. Cooney, G. Ahluwalia, H. Mitsuya, A. Fridland, M. Johnson, Z. Hao, M. Dalal, J. Balzarini, S. Broder, and D. G. Johns. *Biochem. Pharmacol.* **36**:1765–1768 (1987).